Chapter 10
Mucus Matters: The Slippery and Complex Surfaces of Fish

Dylan K. Wainwright and George V. Lauder

Abstract Teleost scales are extremely diverse in morphology, with different categories (cycloid, crenate, spinoid, ctenoid) once used to define major groups of fish. We describe these different classical categories of scales and discuss the structure and potential function of small features of scale morphology such as spines, ctenii, radii, and circuli. Modern techniques now make analysis of scale morphology using three-dimensional quantitative data possible. This ability is crucial because many of the hydrodynamic and protective hypotheses concerning the function of scales are dependent on three-dimensional structure. We discuss different techniques to investigate and image the structure of fish scales and skin, and we highlight gel-based surface profilometry as a new valuable tool for studying fish skin. In addition to bony scales, fish skin is also covered by an epidermis that secretes mucus that can coat the exterior of scales. Fish scales are often studied in isolation with the epidermis removed; here we present topographic, three-dimensional, analyses of fish skin surfaces from seven species with the mucus, epidermis, and relative positions of scales intact. We compare these images qualitatively and quantitatively to the same individuals with the epidermis and mucus removed to show a previously unexplored axis of diversity in fish: how mucus and epidermis interact with scale morphology to create surface texture. The three-dimensional structure of fish skin has important implications for hydrodynamic function during locomotion, but this remains a largely unexplored area.

10.1 Introduction – Fish Surfaces

Fish skin is generally similar to the skin of other vertebrates, with a few important distinctions. Like other vertebrates, fish have an epidermis as their outermost dermal layer and a dermis beneath that, but fish skin is distinguished by the presence of two

D. K. Wainwright (✉) · G. V. Lauder
Department of Organismic and Evolutionary Biology, Harvard University, Cambridge, MA, USA
e-mail: dylanwainwright@fas.harvard.edu

S. N. Gorb, E. V. Gorb (eds.), *Functional Surfaces in Biology III*, Biologically-Inspired Systems 10, https://doi.org/10.1007/978-3-319-74144-4_10

important features – goblet cells full of mucus in the epidermis, and bony scales embedded in the dermis and epidermis (Hawkes 1974; Fast et al. 2002; Zaccone et al. 2001). Other vertebrates may have one of these features, such as bony scales in crocodiles and goblet cells in human mucus membranes, but never both together as in fishes. In teleosts, bony scales appear as overlapping, layered-bone plates embedded in the skin. In this chapter, we will focus on fish surfaces composed of elasmoid scales, thereby excluding both the ganoid scales of basal fish groups (gars and polypterids) and the placoid scales of sharks and rays (Meyer and Seegers 2012; Motta et al. 2012).

Scales likely serve a number of functions in fishes, including physical protection from predators and parasites, prevention of surface fouling, and modification of flow during swimming. However, scales are only a part of a fish's surface, and in fact, scales are not even the outermost part of the skin – instead, an epidermis covers scales and secretes a layer of mucus that covers fish (Fig. 10.1) (Whitear 1970). This layer of epidermis and mucus covers scales and is necessary for scale growth, regeneration, and maintenance (Bereiter-Hahn and Zylberberg 1993; Shephard 1994). The mucus layer is also known to be important for immune function in fishes (Shephard 1994; Rakers et al. 2010; Esteban 2012; Xu et al. 2013), and some authors have also suggested that mucus plays a role in modifying flow conditions around fish to increase swimming efficiency (Rosen and Cornford 1971; Daniel 1981; Bernadsky et al. 1993).

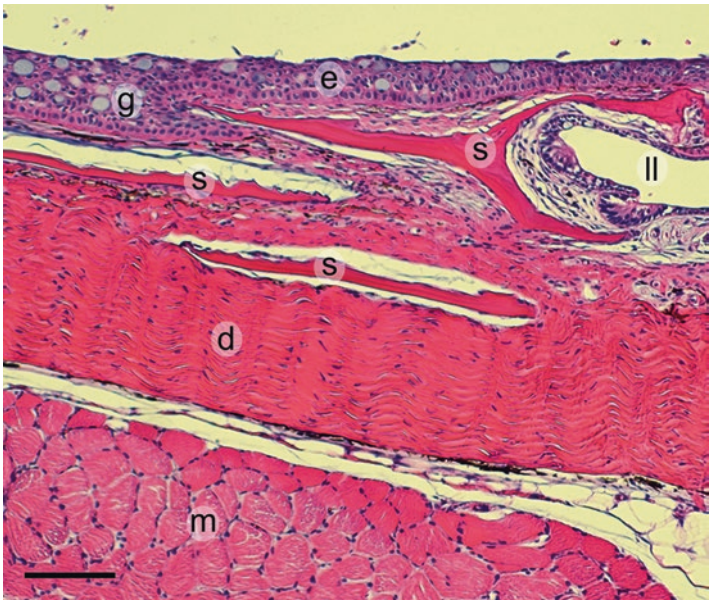

Fig. 10.1 Histological transverse cross-section of skin from a brook trout (*Salvelinus fontinalis*) showing epidermis with goblet cells, scales in scale pockets, and the underlying dermis and muscle. Stained with hematoxylin and eosin. Anterior is coming out of the page, posterior is going into the page. *d* dermis, *e* epidermis, *g* goblet cell, *ll* lateral line canal, *m* muscle, *s* scale. Scale bar: 100 μm

Together, the mucus layer, epidermis, and scales of a fish create the outermost barrier between a fish's body and the external fluid (Fig. 10.1). These tissues also combine to create the topographic texture of a fish's skin. For example, scales overlap in a pattern where the posterior of each scale is inclined towards the outside of the fish, with epidermis and mucus covering the surface of the scales. Scales, epidermis, and mucus interact to create surface topography on the outside of the fish, but the degree to which each of these tissues contributes to topography is unclear. Additionally, structures such as spines, ctenii, and circuli occur on fish scales and create texture on fish (these structures are further discussed below). Fish skin texture in various species has been hypothesized to create favorable flow conditions for swimming by reducing drag, increasing thrust, or increasing efficiency (Bone 1972; Burdak 1986; Liyan et al. 2017); however, these ideas have yet to be tested in a rigorous way. Many ideas about hydrodynamic functions of scales concern how structures on scales, such as spines, can influence the flow around the body of a fish in a favorable way (Burdak 1986; Sagong et al. 2008; Wainwright and Lauder 2016), but these ideas tend to neglect how the epidermis and mucus could also change the topography that the water encounters during swimming.

In this chapter, we will discuss both the diversity of fish scales and how different scale morphologies interact with epidermis and mucus. We will show how mucus changes the topography of fish scale surfaces in a variety of species and elaborate on what that might mean for hypotheses of fish scale function.

10.2 Fish Scales – Complex Surfaces

10.2.1 Scale Types: A Classification

Elasmoid scales of bony fish have three layers (external to internal: limiting layer, external layer, and elasmodine), but the bulk of their structure is elasmodine, a plywood-like structure of collagen fibers that mineralizes into acellular bone with development (Huysseune and Sire 1998; Sire and Huysseune 2003; Meunier 2011). Elasmoid scales are embedded in the epidermis of fishes and are often arranged in an overlapping pattern over the body and sometimes fins. Scales are sheathed in scale pockets, which are connective tissue wrappings that either completely or partially surround the scale (Fig. 10.1) (Bereiter-Hahn and Zylberberg 1993; Sire and Akimenko 2004). Scales grow with the fish – bony fish will replace scales if they fall off or are damaged, but fish do not typically increase the number of scales with growth (Taylor 1916; Thomson 1956; Casselman 1990). Although there is tremendous size diversity in fish scales, scales are routinely 2–15 mm in length, 0.1–2 mm in thickness, and features such as spines and ridges may be tens to hundreds of microns (many exceptions exist to these estimates) (Taylor 1916; Roberts 1993; Wainwright and Lauder 2016; Bergman et al. 2017; Wainwright et al. 2017).

Elasmoid scales of most teleosts have been categorized into different types according to their morphology, with the four main types being cycloid, crenate,

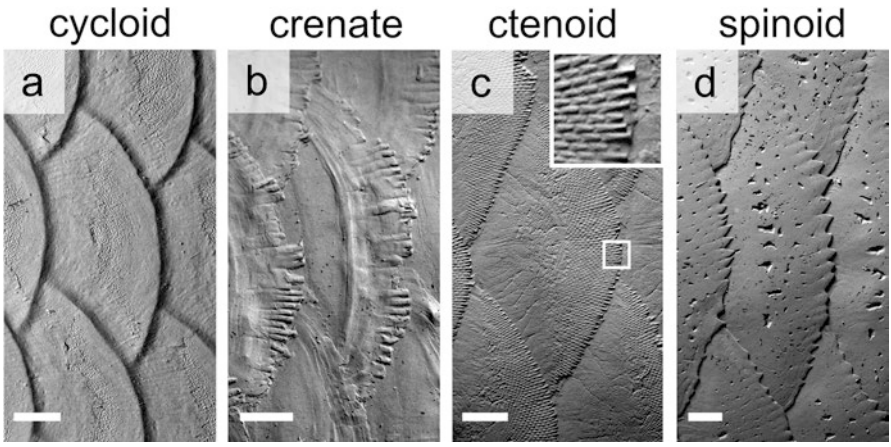

Fig. 10.2 Scale types of teleost fishes illustrated using gel-based profilometry. (**a**) Cycloid scales of bonefish (*Albula vulpes*) with smooth edges. (**b**) Crenate scales of Chacunda gizzard shad (*Anodontostoma chacunda*) with flat, finger-like projections at the posterior edge. (**c**) Ctenoid scales of blackspot sergeant (*Abudefduf sordidus*) with small interlocking spines, enlarged in inset. (**d**) Spinoid scales of sabre squirrelfish (*Sargocentron spiniferum*) with large, flattened, continuous spines. Scale bars: 1 mm

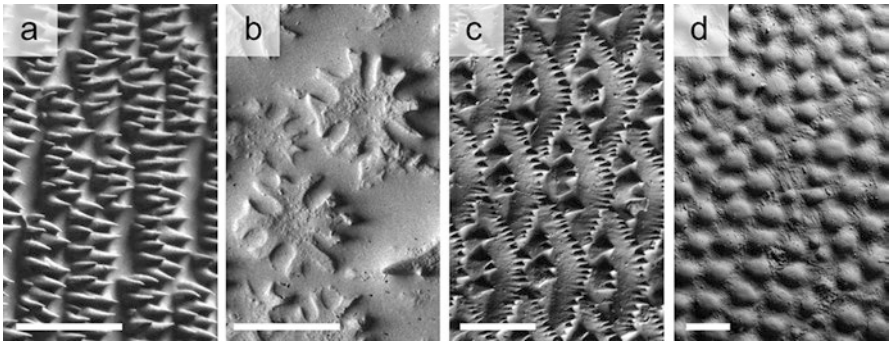

Fig. 10.3 Diversity of fish scales illustrated with gel-based profilometry. (**a**) Complex spiny scales of Moorish idol (*Zanclus cornutus*). (**b**) Oak-leaf-shaped scales of louvar (*Luvarus imperialis*). (**c**) Spiny scales of deepbody boarfish (*Antigonia capros*). (**d**) Interlocking plate-like bumpy scales of scrawled cowfish (*Acanthostracion quadricornis*). Scale bars: 1 mm

ctenoid, and spinoid (Roberts 1993). Figure 10.2 illustrates these four different categories of scales with typical examples of each category. Cycloid scales have smooth posterior edges, crenate scales have edges with flat, blunt projections, ctenoid scales have posterior edges made of separate ossified interlocking spines called ctenii (plural; Fig. 10.2c inset), and spinoid scales have spines that are continuous with the ossification of the scale itself (Roberts 1993).

As is often the case in biology, these classifications hold for large portions of diversity, but there are many exceptions. In Fig. 10.3, we show images of four dif-

ferent fish skin surfaces that illustrate some of the challenges to scale classification. In Fig. 10.3a, we show scales of the Moorish idol (*Zanclus cornuta*) that have many densely-packed spines. We would classify these scales as spinoid because they have spines that are continuous with the ossification of the scale plate themselves, but these look markedly different from the spinoid scales in Fig. 10.2d. Similarly, Fig. 10.3c shows spinoid scales from the boarfish (*Antigonia capros*), which have both spines on the posterior margin of the scale and on the body of the scale. Figure 10.3a, c illustrate how diverse spinoid scales are – so diverse that the classification of spinoid seems to be too broad to have much meaning. C. Roberts (Roberts 1993) remedied this by further classifying scales into subtypes within the different categories, especially in the case of spinoid and ctenoid scales. However, this author also acknowledged how little we know about the evolution and development of different scale types – both of which are relevant to making meaningful categorizations. We also know little about how scale morphology correlates with function, which would inform categorization based not only on morphology, but also on the relationship between morphology and function.

Figure 10.3b shows the bizarre, leaf-shaped scales of a juvenile louvar (*Luvaris imperialis*). These louvar scales are so modified that they do not fit in any current category of scale classification – they are vaguely oak leaf-shaped and sit atop pedestals connected to the rest of the body of the scale. In Fig. 10.3d, the thickened and sutured scales in the scrawled cowfish (*Acanthostracion quadricornis*) are also modified to the point that they defy classification into normal categories and as such, they are often referred to as scutes or dermal plates instead of scales (Besseau and Bouligand 1998). The four species in Fig. 10.3 illustrate a small part of the vast diversity of scales found in different species of fish. It is important that we continue to explore scale diversity in both qualitative and quantitative studies to gain a better understanding of the morphological disparity of scales, the evolutionary patterns of scale morphology, and scale structure-function relationships.

10.2.2 Hypotheses for Functional Diversity in Scales

Although scale morphology is diverse, there are some structural features that are common to most scaled species. We have briefly mentioned some of the microstructures on fish scales above, such as the interlocking ctenii of ctenoid scales and the spines of spinoid scales, but there are other relevant structures like circuli and radii that also occur on many scales. Below we discuss these structural features and potential functions for them.

Circuli are concentric circles usually starting from the scale's center (called the focus), and that represent periods of growth of a scale (similar to tree rings) (Fig. 10.4). They are raised above the surface of the scale and are present on the external surface of scales, facing the water. In many studies, circuli are used to estimate the age of fish, although not by a direct count (Batts 1964; Beardsley 1967; Hill et al. 1989); instead some circuli (called annuli) are closer together and represent

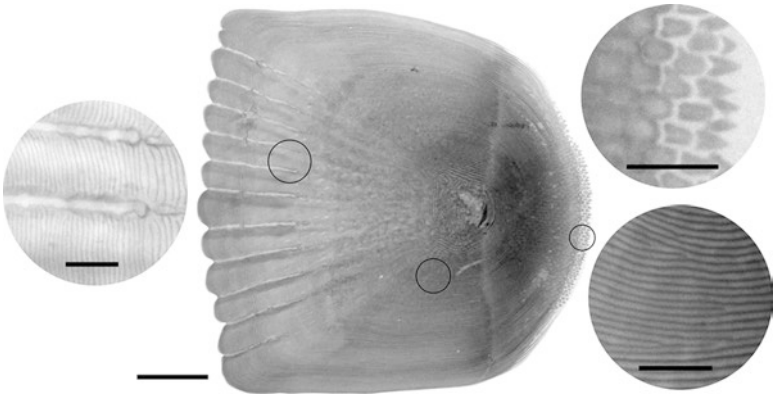

Fig. 10.4 Common features of fish scales. A single cleared and stained scale from a bluegill is shown, anterior to the left and dorsal above. Left inset shows radii, which appear as gaps in the mineralized layers of the scale. Top right inset shows ctenii, which are separate ossified spines that occur at the edge of ctenoid scales. In this scale, the outermost two rows of ctenii are separate mineralizations from the body of the scale, while the other inner (and older) rows of ctenii become mineralized together. Bottom right inset shows circuli, which are concentric ridges on the surface of scales. Scale bar for center image: 1 mm. Scale bars for insets: 200 μm

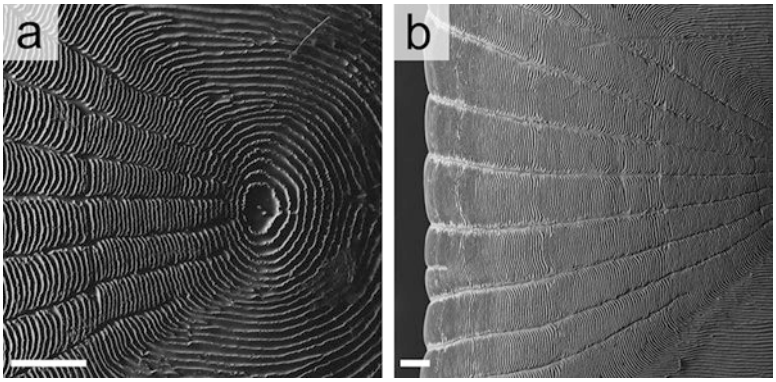

Fig. 10.5 Images of bluegill (*Lepomis macrochirus*) scales taken with scanning electron microscopy (SEM). Anterior is to the left. (**a**) The concentric raised ridges called circuli are clearly visible starting from the focus. Radii are also evident on the anterior part of the scale (left) as breaks in the circuli that radiate from the center to the edge of the scale. (**b**) The anterior margin of the scale with the radii is shown. Scale bars 200 μm (Images credited to James Weaver)

a yearly mark. Circuli can be seen clearly in Figs. 10.4 and 10.5a as they grow around the center of a bluegill scale.

Radii are radial breaks in the mineralization of the scale (but not the unmineralized tissues; Schönbörner et al. 1979) that look like physical gaps in CT scans and cleared and stained scales (Fig. 10.4) or cracks in SEM (Fig. 10.5). Radii are visible in most fish only when the scale is removed from the body because they occur on the anterior

portion of the scale, which is normally covered and layered below more anterior scales (Roberts 1993; Esmaeili et al. 2012). However, some species have radii on the dorsal and ventral regions of the scale (the lateral fields) (e.g. Daniels 1996).

Ctenii are spines that come in a variety of sizes and shapes, and it is often the case that most of the visible portion of the scale (called the posterior field) is made of interlocking ctenii. In these cases, usually only the posterior-most one or two rows of ctenii are whole spines, while the other older ctenii are reduced to shortened interlocking stubs, as shown in Fig. 10.4 (Roberts 1993). The further towards the outer scale margin ctenii are, the younger they are – similar to circuli which grow around the scale center as the scale grows at the edge (Sire 1986; Sire and Arnulf 1990). Because ctenii are separate ossifications from the body of the scale (Fig. 10.4), they may be flexible and can potentially bend relative to the body of the scale to either point externally or internally.

Circuli, radii, ctenii, spines, and other scale features such as overall shape suggest a host of different hypotheses concerning scale function. We have discussed multiple hypotheses for scale structure-function relationships previously (Wainwright and Lauder 2016) and we will summarize several here. Ctenii, spines, circuli, radii, scale shape, and scale curvature may all result in changes in scale stiffness compared to scales without these features. For example, flexibility may be added by fields of separate spiny ctenii, as well as by radii. Increased scale flexibility could benefit undulatory swimmers by decreasing the force needed to bend the scales and skin. Stiffness may be increased using circuli that increase the second moment of area of a scale or by adding curvature to scales, which creates anisotropic stiffness by increasing the second moment of area with respect to different bending axes. Increasing the stiffness of scales could be beneficial for functions like physical protection – creating a scale resistant to bending with little material allows for economical armor.

Fish scales and their features have also been proposed to function hydrodynamically in swimming, with flow being directed in a beneficial way by scale surface structures (Burdak 1986; Wainwright and Lauder 2016; Lauder et al. 2016). Circuli, ctenii, spines of spinoid scales, and scale pattern may either generate turbulence or control turbulence in ways that decrease the overall drag on a fish's body (Anderson et al. 2001; Wainwright and Lauder 2016; Liyan et al. 2017). These fluid mechanisms are dependent on many factors including flow speed, fish size and shape, swimming kinematics, and scale morphology, making it very difficult to investigate the hydrodynamic roles of scale surface structures in these dynamic, small-scale, and species-specific systems. There have been some attempts to assign hydrodynamic functions to fish scales (Aleyev 1977; Burdak 1986; Sagong et al. 2008; Liyan et al. 2017), but these studies either do not present quantitative results or do not test real fish skin. We still know little about how fish surfaces impact the flow around them, and in fact we know little in general about the boundary layer flows around swimming fish (although see Anderson et al. 2001, Yanase and Saarenrinne 2015).

In addition to a potential hydrodynamic role, the microroughness of fish scales created by circuli and ctenii may also function to hold the epidermis and mucus on scales. Covering circuli and ctenii with mucus would make the fish's surface

smoother, which could act to either maintain laminar flow close to the body or prevent boundary layer separation, thereby reducing surface friction (Daniel 1981; Bernadsky et al. 1993). In this case, perhaps fish skin satisfies immune and hydrodynamic functions through the epidermis and mucus, and creates physical protection with bony scales. The functional hypotheses we have outlined above are in no way an exhaustive list of fish scale function and certainly different species may utilize scales and skin in different ways. Furthermore, scales, epidermis, and mucus are undoubtedly a system with multiple biological functions and many of the potential functions of fish skin mentioned above could occur together.

Because of our lack of knowledge tying particular scale morphologies to function, it is important to continue to investigate scale morphology so that we can better understand the diversity of scales and begin to understand how different scales may influence interactions between a fish and its environment. To do this, we first need to understand scale structure in both two and three dimensions to build a strong foundation for testing hypotheses of scale function. Hydrodynamic interactions happen in three dimensions, making it necessary for us to understand the surface topography of scaled surfaces before theorizing about mechanisms fish scales may employ to alter flow during locomotion. This includes the need for additional study of mucus on fish skin and *in vivo* fish surfaces, as seen below in Sect. 10.3.

10.2.3 Investigating Scales – SEM, μCT, Histology, and Profilometry

Studying fish scales and fish skin requires techniques that are able to image sizes in the micron to centimeter range and detect tissues from mucus to bone, which exhibit a range of material and optical properties, and different degrees of hydration. Not many techniques can accomplish all of these at once, but researchers have used optical microscopy, scanning electron microscopy (SEM), micro x-ray computed tomography (μCT), histology, and profilometry to study fish scales and skin. We will briefly discuss some of the benefits of SEM, μCT, histology, and profilometry below. To our knowledge, few studies to date have used μCT and profilometry on fish skin and scales to generate three-dimensional data (Sudo et al. 2002; Wainwright and Lauder 2016; Lauder et al. 2016; Wainwright et al. 2017) – historically, SEM and histology have been the most common approaches to the study of fish skin.

SEM has been a popular way to image and measure scale features for decades and has produced many valuable scale descriptions that reveal patterns of scale evolution and detailed two-dimensional scale morphology of particular species (e.g. Roberts 1993; Johal et al. 2006; Jawad and Al-Jufaili 2007; Sankar et al. 2008; Esmaeili et al. 2012). SEM is an effective technique for investigating scale microstructures such as ctenii, radii, and circuli (Sire and Arnulf 2000; Sire and Huysseune 2003; Meunier and Brito 2004), especially when epidermis and mucus coatings have been removed using dehydration and sample preparation. SEM has also been used to investigate the plywood-like arrangement of fibers in the elasmodine layer

of scales (Meunier 1981; Zylberberg et al. 1988). SEM benefits from fields of view anywhere from a few square micrometers to a few square millimeters and reveals surface details within this range to great effect. However, SEM usually requires specimen preparation (drying, sputter coating) and traditionally only offers two-dimensional information (although environmental SEM requires less specimen preparation). Thus, SEM is not a good technique for understanding the topography of scales or mucus-covered surfaces, but it is a good technique for observing fine details on scale surfaces. Figure 10.5 shows some examples of SEM images of bluegill (*Lepomis macrochirus*) scales, which clearly demonstrate the radii and circuli.

μCT has become an increasingly widespread technique used in research to obtain three-dimensional information about morphology. Because μCT uses x-ray projections to reconstruct morphology, it works best on mineralized biological tissues like bone and shell, although there are now several effective techniques for staining soft tissues with metal ions to enhance CT scan contrast of neural tissue, connective tissues, and muscle (e.g. Descamps et al. 2014; Gignac et al. 2016). Scales are mineralized and thus make good specimens for μCT analysis and the average laboratory μCT resolution of 5–50 microns is within the appropriate range for imaging most fish scales. μCT scans are excellent for reconstructing the full three-dimensionality of scale shape and larger scale features, and they provide a good mechanism for developing computer and physical models of fish scales that could be tested in various experimental and simulation approaches in the future. One downside of laboratory μCT is that this technique is not particularly good at reconstructing the smallest surface features of scales such as individual ctenii or circuli (Wainwright and Lauder 2016). Reconstructing surface renderings of x-ray slices at typical resolutions of 5–50 micron voxel size tends to smooth out small features such as circuli and small ctenii, and the degree of surface roughness is greatly affected by the quality of the render and the values used for thresholding gray values to create the surface.

However, for investigating the volume, structure, and shape of scales in three dimensions, μCT is a good technique to use. We show an example of μCT scans of scales from two different species in Fig. 10.6, illustrating the three-dimensional nature of the data generated with this approach, which can produce three-dimensional surfaces and two-dimensional cross sections through different anatomical planes. Such cross-sectional views are useful for visualizing the relative placement of groups of scales *in situ*, the degree of scale overlap, and the nature of inter-scale connections and contact (Fig. 10.6).

Histology is a tool for investigating scale internal structure and it has the benefit of imaging both soft and hard tissues. Although histological sections can be used as image stacks to reconstruct morphology in three dimensions, it is traditionally a two-dimensional technique. Histology allows us to gain an understanding of relative position of scales and associated soft tissues, and it provides a wealth of information about the structure and composition of different tissues. Compared to SEM and μCT, histology is excellent at displaying soft tissues like the epidermis of fish and goblet cells filled with mucus (Fig. 10.7). Furthermore, histology also provides a method to measure the relative thickness of different skin elements in different species and to generally inspect the structure of the dermis, scales, epidermis, and

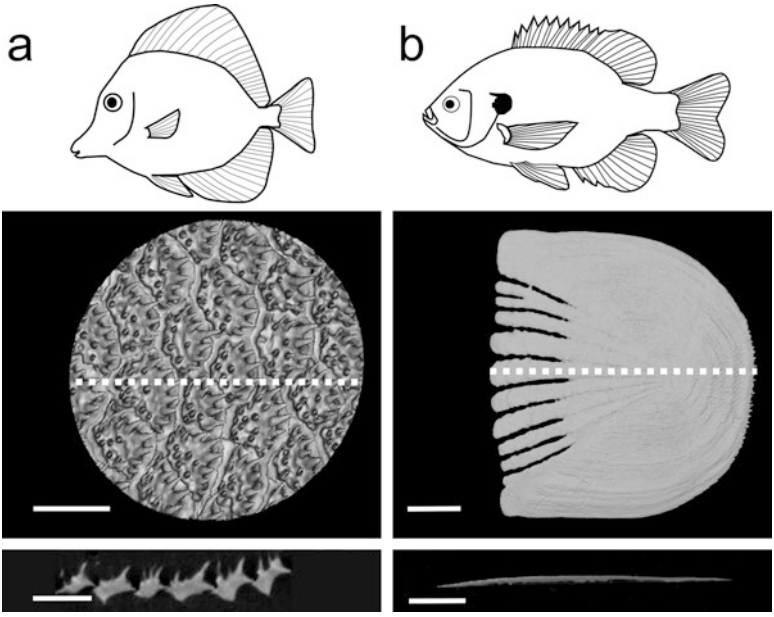

Fig. 10.6 Surface renderings and cross-sections of scales from two species illustrated with models generated from μCT. (**a**) Scales from the yellow tang (*Zebrasoma flavescens*) are shown in a surface rendering containing over 20 scales. A cross-section also shows the three-dimensional nature of these scales and the complex surface texture. (**b**) A scale from a bluegill (*Lepomis macrochirus*) with typical teleost scale morphology. Gaps on the anterior edge are radii, and ctenii are visible on the posterior edge. Cross sectional view below shows that the scale is a single bony plate; note also substantial differences in scale size between these two species. Scale bars: 1 mm

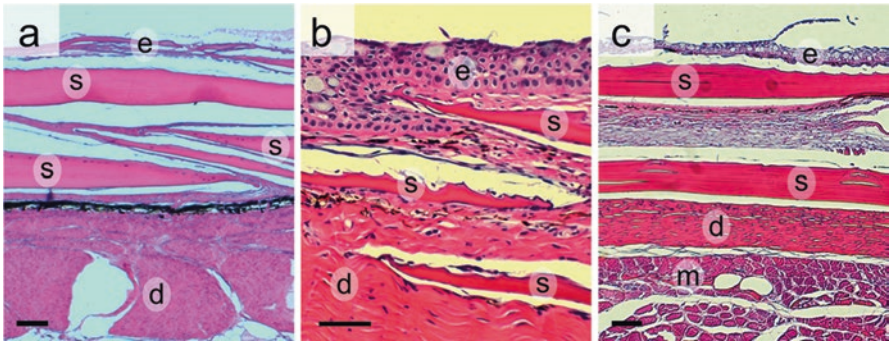

Fig. 10.7 Histological sections of skin and scales for three different fish species. Each sample is stained with hematoxylin and eosin. (**a**) Bigeye tuna (*Thunnus obesus*) has 200 μm thick scales but only a very thin epidermal layer. A dark layer of pigmented tissue is visible above the connective tissue of the dermis. (**b**) Brook trout (*Salvelinus fontinalis*) has a thick epidermis with many goblet cells and thin scales embedded in scale pockets. (**c**) Bluegill (*Lepomis macrochirus*) shows a clear epidermis above and between scales. The dermis lies external to deeper muscle fibers. d: dermis, e: epidermis, m: muscle fibers, s: bony scales. Scale bars: 100 μm

underlying muscle. Disadvantages of histology include difficulty in reconstructing accurate 3D information from slice data and challenges in sectioning fish skin, due to the proximity and location of soft, delicate tissue (epidermis) that is external to hard mineralized tissue (scales). We show histological sections through the skin from three species in Fig. 10.7 to highlight selected structural differences among these species. The relative thickness of the epidermis, scales, and dermis is different in each species, even when the general pattern of bony scales embedded in the dermis remains similar.

For research on fish surface topography, we have found that gel-based surface profilometry (described below) is an excellent method for capturing details of fish surfaces in three dimensions, regardless of skin optical or material properties and without the need for specimen preparation (Wainwright et al. 2017). We use a gel-based profilometry system manufactured by GelSight Inc. (Waltham, MA) that takes images through clear flexible gels pressed onto a surface of interest (Johnson and Adelson 2009; Johnson et al. 2011; Li and Adelson 2013). The contact surface of these clear gels has an opaque coating that standardizes the optical properties of the surface. Six photographs are taken of each surface using a different lighting angle for each image. These photographs are then reconstructed into a three-dimensional topographic map of the surface, which can be quantified using surface metrology metrics such as root-mean-square roughness (Table 10.1). This method

Table 10.1 Root mean square roughness (Sq) values for the nine species in Figs. 10.2, 10.3 and 10.7. Common manufactured surfaces are included for reference

Surface	Roughness Sq (μm)
Extruded aluminum	0.06
1000 grit sandpaper	6.3
Back of hand (*Homo sapiens*)	14.3
Moorish Idol (*Zanclus cornuta*)	14.9
500 grit sandpaper	16.2
Bonefish (*Albula vulpes*)	17.9
Shad (*Anodontosoma chacunda*)	20
Sergeant (*Abudefduf sordidus*)	25.2
Smelt (*Osmerus mordax*)	26.1
Squirrelfish (*Sargocentron spiniferum*)	30.1
Boarfish (*Antigonia capros*)	32.7
Cowfish (*Acanthostracion quadricornis*)	38.6
80 grit sandpaper	53.6
Louvar (*Luvaris imperialis*)	76.5

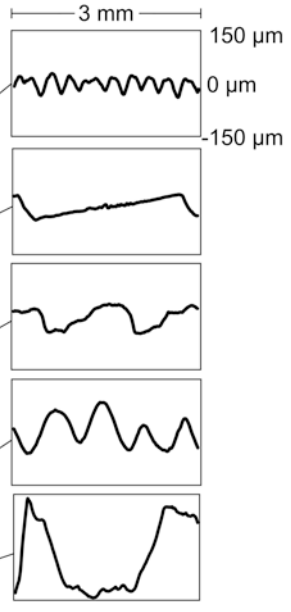

allows for the study of skin on living (anesthetized) fishes, providing a means of understanding the effect of the mucus coating over the surface of scales.

Gel-based profilometry provides significant advantages for studying fish surfaces involved in interactions with the environment because it can reconstruct surfaces in three dimensions, and because this technique can image large fields of view (square centimeters to square millimeters) at high spatial resolutions (each topographic image represents over 18 million three-dimensional points in *x, y,* and *z*). The high-throughput and non-invasive nature of this technique also allows for the study of living animals with the mucus coating intact. Three-dimensional surface data are crucial to furthering the study of hypotheses regarding hydrodynamic function, and techniques like gel-based profilometry allow us to quickly gather this topographic data without damaging or destroying specimens.

We show a reconstruction of the surface of a rainbow smelt (*Osmerus mordax*) from gel-based profilometry and analysis using MountainsMap 7 (Digital Surf Inc., Besançon, France). In Figs. 10.8 and 10.9 displaying this technique, warmer colors correspond to higher elevations on the surface. Using surface profilometry data, elevation profiles can be easily created for analyzing specific surface features, and the surface itself can be used to calculate a large number of canonical surface metrology parameters. We have calculated root-mean-square roughness (Sq) of

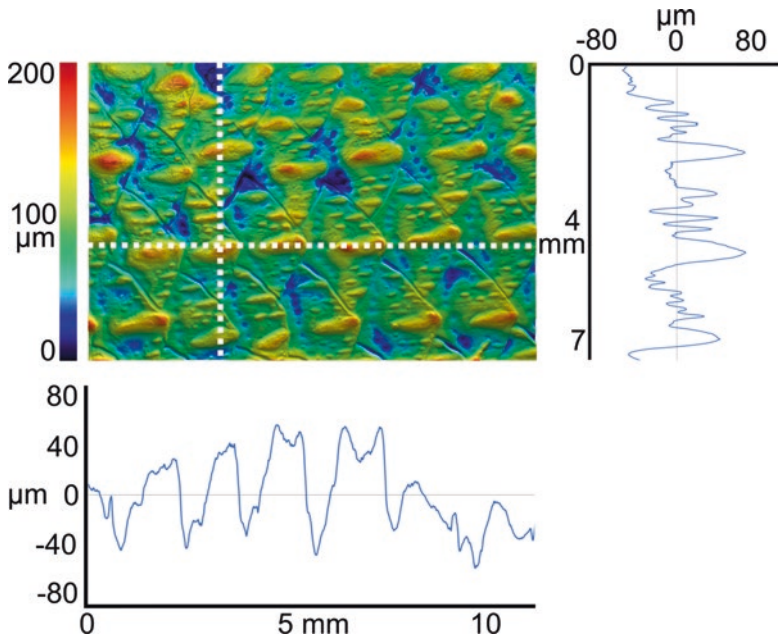

Fig. 10.8 Topographic surface of scales from a rainbow smelt (*Osmerus mordax*) reconstructed using gel-based profilometry. Color refers to elevation, with red colors being highest above the surface. Two orthogonal profile lines are shown to illustrate the three-dimensional nature of these surface data

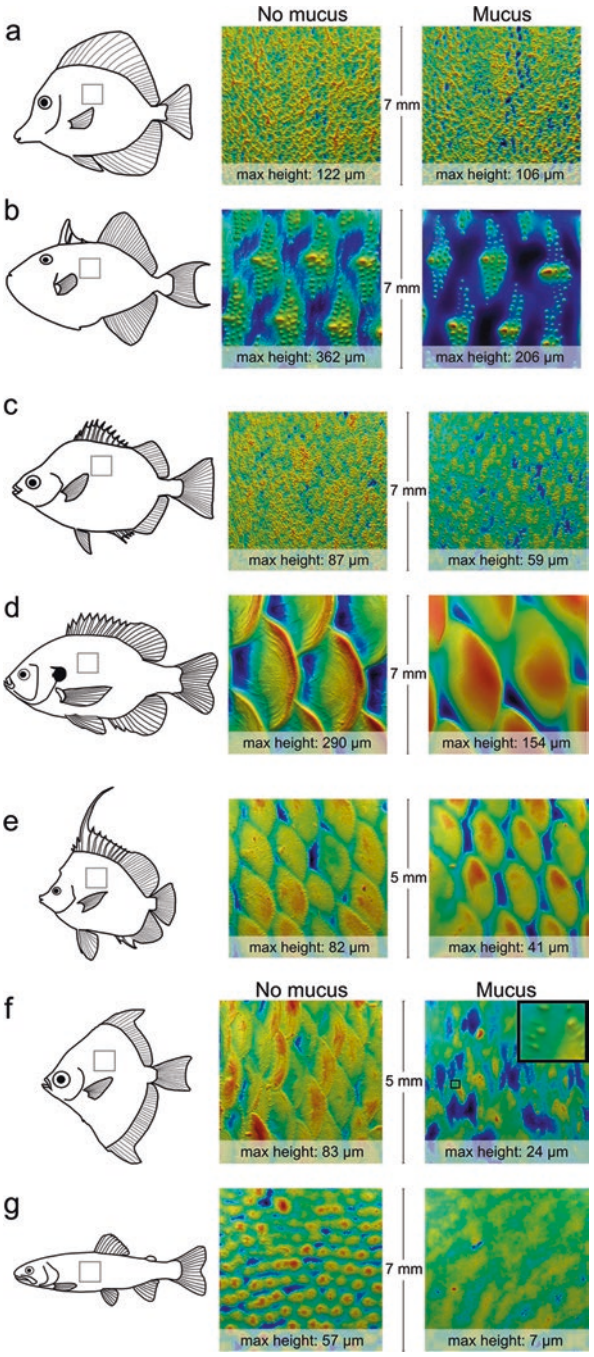

Fig. 10.9 The effect of mucus on fish surface topography. (**a**) Yellow tang (*Zebrasoma flavescens*). (**b**) Niger triggerfish (*Odonus niger*). (**c**) Spotbanded scat (*Selenotoca multifasciatus*). (**d**) Bluegill (*Lepomis macrochirus*). (**e**) Singular bannerfish (*Heniochus singularis*). (**f**) African moony (*Monodactylus sebae*). (**g**) Brook trout (*Salvelinus fontinalis*)

many fish surfaces as well as some manufactured surfaces (extruded aluminum and various sandpapers). Sq represents an average distance a point is from the mean height of the surface. The Sq parameter is calculated by taking a mean height of the surface and then for each point on the surface, subtracting its value from the mean height. These differences between the point and the mean are then squared, integrated across all of the points on the surface, and averaged. Finally, this integrated average value is square-rooted to account for squaring the differences in height. Table 10.1 shows Sq roughness values for several different species of fish discussed in this chapter compared to some manufactured materials. Many other surface metrology parameters exist that describe other topographic qualities. We have previously used skew and kurtosis (which describe the distribution of heights over a surface), max height (another measure of roughness), and texture direction (which evaluates the direction of dominant topographic patterns) (Wainwright and Lauder 2016; Wainwright et al. 2017), but there are an additional 20–30 common surface metrology parameters used in a variety of applications (Whitehouse 1994). We can use these numerous parameters to search for functional traits of fish scales by studying how parameters such as Sq roughness change with different fish that exhibit different behaviors or levels of swimming performance.

10.3 Slippery Surfaces – How Mucus Changes Fish Skin Texture

10.3.1 Fish Surfaces with Mucus

We have previously demonstrated how gel-based profilometry can be used to image the mucus and epidermis that covers scales on anesthetized fishes (Wainwright et al. 2017) and here we present data including *in vivo* surface images from seven different species: yellow tang (*Zebrasoma flavescens*), niger triggerfish (*Odonus niger*), spotbanded scat (*Selenotoca multifasciatus*), bluegill sunfish (*Lepomis macrochirus*), singular bannerfish (*Heniochus singularis*), African moonys (*Monodactylus sebae*), and brook trout (*Salvelinus fontinalis*). We used gel-based profilometry to image the lateral midbody and the peduncle region on each living fish after anesthetizing them with tricaine methanesulfonate (MS-222). We then preserved each individual in a 3.4% formalin solution and imaged the surface again after brushing the surface to remove preserved mucus and epidermis. We imaged one individual of each species in this manner.

We present images of the surfaces both with and without mucus of each species imaged in Fig. 10.9. Note that each image has a different elevation range and we give the maximum height (the elevation value that corresponds to the darkest red) for each image. We have ordered the presentation of these seven species to illustrate how mucus can change the apparent features created by fish scales. The yellow tang in Fig. 10.9a has a surface that changes very little with the presence of mucus and

epidermis. Yellow tangs have scales made of many small laterally projecting spines that protrude clearly above the mucus layer so removing mucus has little effect on the overall topography of their surfaces (Fig. 10.6a also shows yellow tang scales). The niger triggerfish (Fig. 10.9b) and spotband scat (Fig. 10.9c) show similar trends but at different sizes. Both species have raised portions of their scales that clearly protrude past the mucus layer when it is present. However, the boundaries of individual scales are only clear when mucus is removed (i.e. mucus fills the surface and obscures the scale boundaries).

In Fig. 10.9d and e, we show surfaces from a bluegill and a bannerfish, which have similar patterns with and without mucus. Without mucus, the scales of both species are obvious, as are small features on the scale surfaces such as ctenii at the margin and circuli on the body of the scale. However, mucus and the epidermis obscure these small features when present, and instead only the general shape of the scale is obvious in our images with mucus present. Next, we show the surfaces of the moony, which has small scales with ctenii at the posterior margin (Fig. 10.9f). These scales become almost completely obscured in the presence of mucus and epidermis, and instead the only visible features are the small ctenii at the posterior margin of each scale (inset in Fig. 10.9f). Finally, we show how the brook trout's surface changes with and without mucus: trout have small smooth-edged cycloid scales that become completely covered when the epidermis and mucus layers are intact in anesthetized specimens, and maximum surface height is only 7 μm (Fig. 10.9g).

From tang to trout, we see a clear gradient of increasing changes to surface topography with the presence of mucus; yellow tang have surfaces that are very similar with or without mucus, and in contrast, trout scales are completely concealed by mucus. Fish in the middle of this gradient either have scale microstructures obscured (bluegill, bannerfish), scale boundaries obscured (trigger, scat), or most of the scales obscured, and only a few features visible (moony) when mucus and epidermis are present. We also measured the roughness of these seven species with and without mucus and compare values in Table 10.2. We show both quantitatively (Table 10.2) and qualitatively (Fig. 10.9) that surfaces without mucus are rougher than those with mucus, yet there is considerable diversity in this effect. The yellow tang has the smallest decrease in roughness with a 0% change (although the peduncle region of the yellow tang actually shows a curious increase in roughness with mucus) while the trout has the largest percentage decrease in roughness, with a 93% loss. A nominal range from a 0% to a 93% drop in roughness illustrates a challenge of studying fish surfaces – sometimes mucus matters a great deal, but other times it has little effect on surface roughness. We are puzzled by the increase in roughness measured on the yellow tang peduncle scales with mucus compared to without mucus, but we believe this could result from having flexible scales before preservation, that when pressed, will rotate to have spines elevated in line with the z-axis of our measurements, creating higher roughness (whereas in preserved specimens, the scales are fixed and no longer flexible in the skin).

Table 10.2 Roughness of fish surfaces with and without mucus at mid-lateral body (shown in Fig. 10.9) and peduncle positions

Species	Location	No mucus roughness Sq (μm)	Mucus roughness Sq (μm)
Tang	Body	15.2	15.2
	Peduncle	26.0	36.9
Triggerfish	Body	38.7	21.8
	Peduncle	43.5	43.5
Scat	Body	10.9	6.2
	Peduncle	13.9	7.4
Bluegill	Body	55.7	33.5
	Peduncle	61.5	40.8
Bannerfish	Body	10.8	6.9
	Peduncle	9.5	4.4
Moony	Body	11.0	2.7
	Peduncle	11.5	6.1
Trout	Body	8.6	0.6
	Peduncle	10.3	3.9

10.3.2 What Mucus Means for Hypotheses of Function

Mucus has long been considered an important part of fish swimming (Daniel 1981; Bernadsky et al. 1993), and our topographic data have important implications for how fish surfaces may function hydrodynamically, as mucus clearly alters surface roughness and the effect of mucus in obscuring surface roughness changes along the body (Table 10.2). Furthermore, there is not necessarily a correlation between the appearance of scales and what those scales look like when covered by epidermis and mucus. For example, both the moony (Fig. 10.9f) and the bannerfish (Fig. 10.9e) have similar size and elevated features on their scales, but anesthetized specimens with mucus intact appear different in these two species. This indicates that not only does scale morphology differ between species, but so too does the morphology of the epidermis and mucus layers, showing us that the topography of live fish is determined by interactions between scale, epidermis, and mucus morphology.

The interaction between the complex structure of scales and the slippery nature of epidermis and mucus changes many of the hypotheses concerning the function of fish scale morphology. Many of the species we imaged have part or all of their ctenii and circuli completely obscured by epidermal tissues or mucus and thus, it seems that in these species and others like them, ctenii and circuli will not play a role in locomotor hydrodynamics except perhaps an indirect one by holding mucus and epidermis on the surface. However, we do not know if patterns of body bending during swimming might expose ctenii to water flow as scales bend and slide past each other as the body undulates. The effect of body bending patterns on scale relative position and surface feature exposure remains entirely unknown.

One additional complexity is that fish scale morphology changes across a fish's body (e.g. Jawad 2005; Wainwright and Lauder 2016), and we have noted rougher and more rugose scales in the peduncle and other posterior regions in many species that we have investigated (Wainwright and Lauder 2016; Wainwright et al. 2017). Because of this, it is possible that anterior scales or scale features could be covered by mucus and epidermis, but more extreme-featured posterior scales may be less changed by the epidermis and mucus layers. Fluid flow along the body of a fish will change as flow moves from head to tail because of the natural development of boundary layer flow coupled with changes in movement and body shape. It is possible that scales are hidden under mucus on anterior parts of a fish where there is a laminar boundary layer and then protrude into the boundary layer towards the tail to create turbulence and maintain flow attachment.

Functional measurements of how fish scales change boundary layer flow do not exist. There are some measurements of fish boundary layers (Anderson et al. 2001; Yanase and Saarenrinne 2015) and they indicate that swimming fish likely experience both laminar and turbulent boundary layers depending on Reynolds number, fish kinematics, and the region of the fish being investigated. These measurements come from just two species of bony fish, however, and thus cannot provide much information on the effect of scales. In order for us to begin to answer how scales interact with boundary layer flows, we need careful experimental measurements of the boundary layer of fish skin, starting with static conditions and eventually moving towards dynamic testing with flapping skin pieces with and without mucus, and finally to free-swimming fish. To investigate different skin topographies, we need careful choice of fish species to compare not just one species to another, but to compare general scale morphologies against one another. These experiments could also be accomplished with physical models if models are validated as having similar flow properties to fish scales, as has been done in placoid shark scales (Wen et al. 2014; Wen et al. 2015).

Until experiments on boundary layer flow over different fish scale morphologies are completed, we can focus the discussion on scale topography and boundary layer interactions in another way. The engineering parameter k+, also known as roughness Reynolds number (Jimenez 2004), provides an estimate of whether surface roughness will change boundary layer characteristics. k+ values do not estimate whether an effect on the boundary layer will be beneficial or not – they simply estimate if a surface has features that are large enough to change flow in the boundary layer relative to a smooth surface. The k+ parameter is calculated by multiplying friction velocity of the fluid by the height of surface features and dividing by the viscosity of the fluid of interest (Jimenez 2004; Schultz and Flack 2007). Viscosity of salt or freshwater is known, the size of surface features can be measured with gel-based profilometry, and friction velocity can be estimated using power law equations involving the Reynolds number (Smits 2000). Because calculating friction velocity uses the Reynolds number, a known or estimated swimming speed is needed, along with the distance from the anterior tip of the body to the region under investigation. This also means that each k+ value is relevant only for a particular swimming speed and location on the body. k+ values of less than three indicate that

surface features are too small to disturb the boundary layer; values over three indicate that surface features are likely to change the boundary layer flow.

Although the height of surface features is incorporated into k+ estimation, surface geometry and patterning are also important to boundary layer effects and are not taken into account with k+. For example, if two surfaces have the same feature size, but one surface is covered in smooth-sloping ridges while the other is covered in sharp-peaked ridges, the sharp ridges will be more likely to change boundary layer flow because sharp features provide natural separation points on the surface. Aside from ignoring surface geometry, simple calculations of k+ also assume that objects are not moving across the flow, a condition that is violated during undulatory fish swimming, especially on posterior regions of the body. Nonetheless, a cutoff value of three for k+ is sufficiently conservative and our k+ values will give us a guide for future data collection. Questions relating to boundary layer flows on a deforming flexible object with a surface coating are complex, and k+ can provide a useful initial piece of a broader multivariate approach.

We can use k+ as a way of narrowing the field of potential scale functions – if a particular fish's surface has a k+ below three, then its surface features are simply too small to have a substantial effect on the boundary layer. In Fig. 10.10 we present k+ values for the different species in Fig. 10.8 using surface profilometry data and estimates of swimming speed. We include values for surfaces with mucus and for swimming both at one body-length per second and three body lengths per second. We also include values calculated from scale height data at the midbody of each fish (Fig. 10.8) as well as from the peduncle of the fish. Note that these values are for the specific specimens we used in this study and the specific regions we imaged on their body surfaces. Caution should be used before extrapolating these results to larger individuals of the same species or different regions on the same species. Additionally, we are not accounting for either surface geometry (sharpness of corners of edges, spacing between peaks) or body undulation, so our k+ values should be viewed as hypotheses instead of corroborated results.

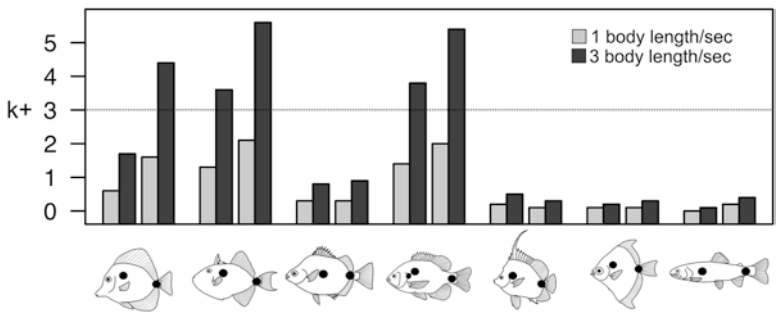

Fig. 10.10 Calculated k+ values of fish with mucus at body and peduncle regions at two different swimming speeds, one and three body lengths per second (see legend). From left to right species, with body region always followed by the peduncle region: yellow tang, niger triggerfish, scat, bluegill, bannerfish, moony, trout. k+ cutoff value of three is marked with a line – values above three indicate surfaces where flow may be altered in the boundary layer

We find that the only fish with k+ values above three are yellow tang, niger triggerfish, and bluegill (Fig. 10.10). These fish have the roughest surfaces among the seven species we investigated (Table 10.2), so it is unsurprising that these are the fish that are most likely to have scales that change the boundary layer flow in some way, even with the presence of mucus and epidermis. Yellow tang has skin with many small distal-pointing spines on their scale surfaces and these spines increase in size at the peduncle, just anterior to the scalpel-like spine also located there. It is these larger spines that are likely the reason the yellow tang shows a k+ over three only on the peduncle at the higher swimming speed of three body lengths per second. The triggerfish has k+ values above three on body and peduncle regions, but only at swimming speeds of three body lengths per second, indicating surface geometry may only affect the boundary layer at high swimming speeds. Bluegill also shows high k+ values on both body and peduncle regions only at the faster swimming speed of three body lengths per second. Calculating k+ provides a way of identifying potential candidates for future experimental studies of boundary layers around swimming fish.

10.4 Concluding Remarks

Fish scales display a vast diversity of morphology – scale size, shape, and internal structure vary among species, different populations of the same species, and on different regions of the same fish (Margraf and Riley 1993; Roberts 1993; Dapar et al. 2012; Wainwright and Lauder 2016). While we have a basic understanding about how scales vary and develop (Suzuki 1971; Roberts 1993; Sire and Akimenko 2004) and we have been able to quantify scales in two dimensions (Ibañez et al. 2007; Ibañez et al. 2009), we have only just begun to understand the surface of scales and fish skin in three dimensions, and we still have no understanding of how scale morphology and deployment changes with fish activity. Gel-based profilometry provides a method of reconstructing the surface topography of scales in different species of fish with the hopes of eventually using this information to elucidate the function of different scale morphologies (Wainwright and Lauder 2016; Lauder et al. 2016; Wainwright et al. 2017). Understanding scale topography in three dimensions is both necessary and important for studying fish scale hydrodynamic function because of the role surface features have in changing boundary layer flows. Furthermore, understanding the three-dimensional morphology of fish scales in a quantitative manner allows for more rigorous exploration of fish surfaces in the contexts of morphology, evolutionary patterns, and the form-function relationship of scales.

We also demonstrated how fish scale topography changes on fish where mucus and skin are still intact atop the scales. Using gel-based profilometry, we have discovered that mucus and epidermis can often obscure and cover small structures present on fish scales, which changes the roughness and structure of a mucus-coated surface compared to a preserved fish without mucus or epidermis. By imaging a diverse sample of seven species, we show that scale morphology alone is a poor predictor of *in vivo* skin topography, and that mucus, epidermis, and scales interact

to form complicated 3D surfaces. Some fish have rough surfaces that are barely changed with the presence of live skin tissues (yellow tang, triggerfish), while others have scales that are completely changed by mucus and epidermis to create a very smooth external surface (trout). It is likely that most fish fall in the middle of this spectrum, with most scale microstructure obscured by mucus but with general scale shape still visible, perhaps also with some spines or ctenii. The imaging and quantitative comparison of mucus-covered fish surfaces is a new area of research and reveals what surfaces are like on living fish, which is vital information for understanding what type of surface the water interacts with during swimming.

Despite promising new techniques to image and quantify fish scale topography, we still know little about fish scale function. Other authors have studied the armor-like aspects of fish scales (Vernerey and Barthelat 2010; Song et al. 2011; Browning et al. 2013; Chintapalli et al. 2014; Vernerey and Barthelat 2014; Duro-Royo et al. 2015), and the roles fish skin have in body and skin bending (Long et al. 1996; Ghosh et al. 2014; Szewciw et al. 2017), yet work on the hydrodynamic effect of fish scales remains hypothetical (Walters 1963; Burdak 1986; Sudo et al. 2002; Liyan et al. 2017). In part, it is challenging to experimentally study fine-scale flows on swimming fish, which is compounded by the fact that we also know little about boundary layer flow around freely-swimming fishes. In order to investigate how and if fish scales change boundary layer flow for better or worse, we can use metrics like k+ to search for surfaces of potential interest, and then investigate function experimentally. Using micro-scale particle image velocimetry with real fish skin pieces, using physical models of scales or fish surfaces, or using phylogenetic comparative methods to link different scale morphologies with ecology or swimming performance are all key areas for future study. The functional implications of the complex and slippery surfaces of fish remains an intriguing and understudied area of fish biology, and with research on scale morphology, surface topography, fluid mechanics, and evolutionary patterns, we can move toward a comprehensive understanding of the form and function of fish surfaces.

Acknowledgements We would like to acknowledge James Weaver for his imaging expertise (in particular for the images in Fig. 10.5), and Kimo Johnson for his assistance with GelSight profilometry measurements. We acknowledge Karsten Hartel and Andrew Williston with assistance in accessing specimens and Dr. Lex Smits for introducing us to k+. The research reported here was supported by ONR MURI Grant N000141410533 monitored by Dr. Bob Brizzolara, HFSP Young Investigators Grant (RGY0067- 2013) to James Weaver, and NSF GRF 2014162421 awarded to D.K.W.

References

Aleyev, Y. G. (1977). *Nekton*. Hague: Dr. W. Junk b.v. Publishers.

Anderson, E. J., McGillis, W. R., & Grosenbaugh, M. A. (2001). The boundary layer of swimming fish. *The Journal of Experimental Biology, 204*, 81–102.

Batts, B. S. (1964). Lepidology of the adult pleuronectiform fishes of Puget Sound, Washington. *Copeia, 4*, 666–673.

Beardsley, G. L. (1967). Age, growth, and reproduction of the Dolphin, *Coryphaena hippurus*, in the Straits of Florida. *Copeia, 1967*, 441.

Bereiter-Hahn, J., & Zylberberg, L. (1993). Regeneration of teleost fish scale. *Comparative Biochemistry and Physiology, 105A*, 625–641.

Bergman, J. N., Lajeunesse, M. J., & Motta, P. J. (2017). Teeth penetration force of the tiger shark *Galeocerdo cuvier* and sandbar shark *Carcharhinus plumbeus*. *Journal of Fish Biology, 91*, 460–472.

Bernadsky, G., Sar, N., & Rosenberg, E. (1993). Drag reduction of fish skin mucus: Relationship to mode of swimming and size. *Journal of Fish Biology, 42*, 797–800.

Besseau, L., & Bouligand, Y. (1998). The twisted collagen network of the box-fish scutes. *Tissue & Cell, 30*, 251–260.

Bone, Q. (1972). Buoyancy and hydrodynamic functions of integument in the Castor oil fish, *Ruvettus pretiosus* (Pisces: Gempylidae). *Copeia, 1972*, 78–87.

Browning, A., Ortiz, C., & Boyce, M. C. (2013). Mechanics of composite elasmoid fish scale assemblies and their bioinspired analogues. *Journal of the Mechanical Behavior of Biomedical Materials, 19*, 75–86.

Burdak, V. D. (1986). Morphologie fonctionnelle du tegument ecailleux des poissons. *Cybium, 10*, 1–128.

Casselman, J. M. (1990). Growth and relative size of calcified structures of fish growth and relative size of calcified structures of fish. *Transactions of the American Fisheries Society, 119*, 673–688.

Chintapalli, R. K., Mirkhalaf, M., Dastjerdi, A. K., & Barthelat, F. (2014). Fabrication, testing and modeling of a new flexible armor inspired from natural fish scales and osteoderms. *Bioinspiration & Biomimetics, 9*, 36005.

Daniel, T. L. (1981). Fish mucus: In situ measurements of polymer drag reduction. *The Biological Bulletin, 160*, 376–382.

Daniels, R. A. (1996). Guide to the identification of scales of inland fishes of northeastern North America. *New York State Museum Bulletin, 488*, 1–93.

Dapar, M. L. G., Torres, M. A. J., Fabricante, P. K., & Demayo, C. G. (2012). Scale morphology of the Indian goatfish, *Parapeneus indicus* (Shaw, 1803) (Perciformes: Mullidae). *Advance Envirronmental Biologico, 6*, 1426–1432.

Descamps, E., Sochacka, A., de Kegel, B., Van Loo, D., Hoorebeke, L., & Adriaens, D. (2014). Soft tissue discrimination with contrast agents using micro-ct scanning. *Belgian Journal of Zoology, 144*, 20–40.

Duro-Royo, J., Zolotovsky, K., Mogas-Soldevila, L., Varshney, S., Oxman, N., Boyce, M. C., & Ortiz, C. (2015). MetaMesh: A hierarchical computational model for design and fabrication of biomimetic armored surfaces. *Computer-Aided Design, 60*, 14–27.

Esmaeili, H. R., Gholamifard, A., Zarei, N., & Arshadi, A. (2012). Scale structure of a cyprinid fish, *Garra rossica* (Nikol'skii, 1900) using scanning electron microscope (SEM). *International Journal of Science, Technology and Society, 4*, 487–492.

Esteban, M. Á. (2012). An overview of the immunological defenses in fish skin. *ISRN Immunology, 2012*, 1–29.

Fast, M. D., Sims, D. E., Burka, J. F., Mustafa, A., & Ross, N. W. (2002). Skin morphology and humoral non-specific defence parameters of mucus and plasma in rainbow trout, coho and Atlantic salmon. *Comparative Biochemistry and Physiology A, 132*, 645–657.

Ghosh, R., Ebrahimi, H., & Vaziri, A. (2014). Contact kinematics of biomimetic scales. Applied Physics Letters. *105*, 233701-1-233701-5.

Gignac, P. M., Kley, N. J., Clarke, J. A., Colbert, M. W., Morhardt, A. C., Cerio, D., Cost, I. N., Cox, P. G., Daza, J. D., Early, C. M., et al. (2016). Diffusible iodine-based contrast-enhanced computed tomography (diceCT): An emerging tool for rapid, high-resolution, 3-D imaging of metazoan soft tissues. *Journal of Anatomy, 228*, 889–909.

Hawkes, J. W. (1974). The structure of fish skin I. General organization. *Cell and Tissue Research, 149*, 147–158.

Hill, K. T., Cailliet, G. M., & Radtke, R. L. (1989). A comparative analysis of growth zones in four calcified structures of Pacific Blue Marlin, *Makaira nigricans*. *Fishery Bulletin, 87*, 829–843.
Huysseune, A., & Sire, J.-Y. (1998). Evolution of patterns and processes in teeth and tooth-related tissues in non-mammalian vertebrates. *European Journal of Oral Sciences, 106*, 437–481.
Ibañez, A. L., Cowx, I. G., & O'Higgins, P. (2007). Geometric morphometric analysis of fish scales for identifying genera, species, and local populations within the Mugilidae. *Canadian Journal of Fisheries and Aquatic Sciences, 1100*, 1091–1100.
Ibañez, A. L., Cowx, I. G., & O'Higgins, P. (2009). Variation in elasmoid fish scale patterns is informative with regard to taxon and swimming mode. *Zoological Journal of the Linnean Society, 155*, 834–844.
Jawad, L. A. (2005). Comparative scale morphology and squamation patterns in triplefins (Pisces: Teleostei: Perciformes: Tripterygiidae). *Tuhinga, 16*, 137–167.
Jawad, L. A., & Al-Jufaili, S. M. (2007). Scale morphology of greater lizardfish *Saurida tumbil* (Bloch, 1795) (Pisces: Synodontidae). *Journal of Fish Biology, 70*, 1185–1212.
Jimenez, J. (2004). Turbulent flows over rough walls. *Annual Review of Fluid Mechanics, 36*, 173–196.
Johal, M. S., Esmaeili, H. R., & Sharma, M. L. (2006). Scale structure of a cobitid fish, *Cobitis linea* (Heckel, 1849) using different modes of SEM. *Current Science, 91*, 1464–1466.
Johnson, M.K. and Adelson, E.H. (2009). Retrographic sensing for the measurement of surface texture and shape. In: *2009 IEEE Conference on Computer Vision and Pattern Recognition*, 1070–1077.
Johnson, M. K., Cole, F., Raj, A., & Adelson, E. H. (2011). Microgeometry capture using an elastomeric sensor. *ACM Transactions on Graphics, 30*, 46.
Lauder, G. V., Wainwright, D. K., Domel, A. G., Weaver, J., Wen, L., & Bertoldi, K. (2016). Structure, biomimetics, and fluid dynamics of fish skin surfaces. *Physical Review Fluids, 1*, 060502.
Li, R., & Adelson, E. H. (2013). Sensing and recognizing surface textures using a GelSight sensor. In: *2013 IEEE Conference on Computer Vision and Pattern Recognition*, pp. 1241–1247.
Liyan, W. U., Zhibin, J., Yuqiu, S., Wentao, R., Shichao, N., & Zhiwu, H. (2017). Water-trapping and drag-reduction effects of fish *Ctenopharyngodon idellus* scales and their simulations. *Science China Technological Sciences, 60*, 1111–1117.
Long, J. H., Hale, M. E., McHenry, M. J., & Westneat, M. W. (1996). Functions of fish skin: Flexural stiffness and steady swimming of longnose gar *Lepisosteus osseus*. *The Journal of Experimental Biology, 199*, 2139–2151.
Margraf, F. J., & Riley, L. M. (1993). Evaluation of scale shape for identifying spawning stocks of coastal Atlantic striped bass (*Morone saxatilis*). *Fisheries Research, 18*, 163–172.
Meunier, F. J. (1981). "Twisted plywood" structure and mineralization in the scales of a primitive living fish *Amia calva*. *Tissue & Cell, 13*, 165–171.
Meunier, F. J. (2011). The Osteichtyes, from the Paleozoic to the extant time, through histology and palaeohistology of bony tissues. *Comptes Rendus Palevol, 10*, 347–355.
Meunier, F. J., & Brito, P. M. (2004). Histology and morphology of the scales in some extinct and extant teleosts. *Cybium, 28*, 225–235.
Meyer, W., & Seegers, U. (2012). Basics of skin structure and function in elasmobranchs: A review. *Journal of Fish Biology, 80*, 1940–1967.
Motta, P., Habegger, M. L., Lang, A., Hueter, R., & Davis, J. (2012). Scale morphology and flexibility in the shortfin mako *Isurus oxyrinchus* and the blacktip shark *Carcharhinus limbatus*. *Journal of Morphology, 273*, 1096–1110.
Rakers, S., Gebert, M., Uppalapati, S., Meyer, W., Maderson, P., Sell, A. F., Kruse, C., & Paus, R. (2010). "Fish matters": The relevance of fish skin biology to investigative dermatology. *Experimental Dermatology, 19*, 313–324.
Roberts, C. D. (1993). Comparative morphology of spined scales and their phylogenetic significance in the Teleostei. *Bulletin of Marine Science, 52*, 60–113.
Rosen, M. W., & Cornford, N. E. (1971). Fluid friction of fish slimes. *Nature, 234*, 49–51.

Sagong, W., Kim, C., Choi, S., Jeon, W.-P. and Choi, H. (2008). Does the sailfish skin reduce the skin friction like the shark skin? *Physics of Fluids*, *20*, 101510-1-101510-10.
Sankar, S., Sekar, S., Mohan, R., Rani, S., Sundaraseelan, J., & Sastry, T. P. (2008). Preparation and partial characterization of collagen sheet from fish (*Lates calcarifer*) scales. *International Journal of BIological Macromolecules, 42*, 6–9.
Schönbörner, A. A., Boivin, G., & Baud, C. A. (1979). The mineralization processes in teleost fish scales. *Cell and Tissue Research, 202*, 203–212.
Schultz, M. P., & Flack, K. A. (2007). The rough-wall turbulent boundary layer from the hydraulically smooth to the fully rough regime. *Journal of Fluid Mechanics, 580*, 381.
Shephard, K. L. (1994). Functions for fish mucus. *Reviews in Fish Biology and Fisheries, 4*, 401–429.
Sire, J.-Y. (1986). Ontogenic development scales in a cichlid *Hemichromis bimaculatus* (Cichlidae). *Journal of Fish Biology, 28*, 713–724.
Sire, J.-Y., & Akimenko, M.-A. (2004). Scale development in fish: A review, with description of sonic hedgehog (shh) expression in the zebrafish (*Danio rerio*). *The International Journal of Developmental Biology, 48*, 233–247.
Sire, J.-Y., & Arnulf, I. (1990). The development of squamation in four Teleostean fishes with a survey of the literature. *Jpn. Journal of Ichthyology, 37*, 133–143.
Sire, J., & Arnulf, I. (2000). Structure and development of the ctenial spines on the scales of a teleost fish, the cichlid *Cichlasoma nigrofasciatum*. *Acta Zoologica, 81*, 139–158.
Sire, J.-Y., & Huysseune, A. (2003). Formation of dermal skeletal and dental tissues in fish: A comparative and evolutionary approach. *Biological Reviews of the Cambridge Philosophical Society, 78*, 219–249.
Smits, A. J. (2000). *A physical introduction to fluid mechanics*. New York: John Wiley and Sons.
Song, J., Ortiz, C., & Boyce, M. C. (2011). Threat-protection mechanics of an armored fish. *Journal of the Mechanical Behavior of Biomedical Materials, 4*, 699–712.
Sudo, S., Tsuyuki, K., Ito, Y., & Ikohagi, T. (2002). A study on the surface shape of fish scales. *Trans. Jpn. Soc. Mechanical Engineering, 45*, 1100–1105.
Suzuki, T. (1971). Some scale patterns of the scad, Decapterus maruadsi (Temminck et Schlegel), and their variations with body parts. *Bulletin of the Japan Sea Regional Fisheries Research Laboratory 23*, 1–19.
Szewciw, L., Zhu, D., & Barthelat, F. (2017). The nonlinear flexural response of a whole teleost fish: Contribution of scales and skin. *Journal of the Mechanical Behavior of Biomedical Materials, 17*, 30252–30257.
Taylor, H. F. (1916). The structure and growth of the scales of the squeteague and the pigfish as indicative of life history. *Fishery Bulletin, 34*, 285–330.
Thomson, J. M. (1956). Interpretation of the scales of the yellow-eye mullet, *Aldrichetta forsteri* (Cuvier & Valenciennes) (Mugilidae). *Australian Journal of Marine and Freshwater Research, 8*, 14–30.
Vernerey, F. J., & Barthelat, F. (2010). On the mechanics of fishscale structures. *International Journal of Solids and Structures, 47*, 2268–2275.
Vernerey, F. J., & Barthelat, F. (2014). Skin and scales of teleost fish: Simple structure but high performance and multiple functions. *Journal of the Mechanics and Physics of Solids, 68*, 66–76.
Wainwright, D. K., & Lauder, G. V. (2016). Three-dimensional analysis of scale morphology in bluegill sunfish, *Lepomis macrochirus*. *Zoology, 119*, 182–195.
Wainwright, D. K., Lauder, G. V., & Weaver, J. C. (2017). Imaging biological surface topography *in situ* and *in vivo*. *Methods in Ecology and Evolution*. in press.
Walters, V. (1963). The Trachipterid integument and an hypothesis on its hydrodynamic function. *Copeia, 1963*, 260–270.
Wen, L., Weaver, J. C., & Lauder, G. V. (2014). Biomimetic shark skin: Design, fabrication and hydrodynamic function. *The Journal of Experimental Biology, 217*, 1656–1666.

Wen, L., Weaver, J. C., Thornycroft, P. J. M., & Lauder, G. V. (2015). Hydrodynamic function of biomimetic shark skin: Effect of denticle pattern and spacing. *Bioinspiration & Biomimetics, 10*, 066010.

Whitear, M. (1970). The skin surface of bony fishes. *Journal of Zoology, 4*, 437–454.

Whitehouse, D. J. (1994). *Handbook of surface metrology*. Philadelphia: Institute of Physics Publishing.

Xu, Z., Parra, D., Gomez, D., Salinas, I., Zhang, Y.-A., von Gersdorff Jørgensen, L., Heinecke, R. D., Buchmann, K., LaPatra, S., & Sunyer, J. O. (2013). Teleost skin, an ancient mucosal surface that elicits gut-like immune responses. *Proceedings of the National Academy of Sciences of the United States of America, 110*, 13097–13102.

Yanase, K., & Saarenrinne, P. (2015). Unsteady turbulent boundary layers in swimming rainbow trout. *The Journal of Experimental Biology, 218*, 1373–1385.

Zaccone, G., Kapoor, B. G., Fasulo, S., & Ainis, L. (2001). Structural, histochemical and functional aspects of the epidermis of fishes. *Advnces in Marine Biology, 40*, 253–348.

Zylberberg, L., Bereiter-Hahn, J., & Sire, J. Y. (1988). Cytoskeletal organization and collagen orientation in the fish scales. *Cell and Tissue Research, 253*, 597–607.